BCSJ

Document type: Review/Account

Account/Review for Frontiers of Molecular Science

A Short History of Cyclocarbons[#]

Harry L. Anderson,* Connor W. Patrick, Lorel M. Scriven, and Steffen L. Woltering

Department of Chemistry, Oxford University, Chemistry Research Laboratory, Oxford, OX1 3TA, UK

E-mail: harry.anderson@chem.ox.ac.uk

Received: October 30, 2020; Accepted: December 1, 2020; Web Released: December 9, 2020

Harry L. Anderson
Harry L. Anderson received his PhD from the University of Cambridge in 1990. He carried out postdoctoral work on fullerene chemistry with François Diederich at ETH Zurich, Switzerland, before starting his independent group at the University of Oxford in 1995. His fields of research are physical organic and supramolecular chemistry, including aromaticity, carbon-rich materials, rotaxanes, porphyrins, photochromic dyes, template-directed synthesis, multivalent cooperativity and molecular electronics.

Connor W. Patrick
Connor W. Patrick received his first degree in 2018 from the University of Durham, which included a Master's year investigating the spectroscopic properties of lanthanide probes, under the supervision of Professor David Parker. He is currently a PhD student in Harry Anderson's group at the University of Oxford working in the field of supramolecular encapsulation of polyynes and cyclocarbons.

Lorel M. Scriven
Lorel M. Scriven completed an MSc in Natural Sciences at the University of Cambridge in 2017, including a Masters project on signal transduction by molecular transportation in vesicles under the supervision of Professor Christopher Hunter. She is currently a PhD student in Harry Anderson's group at the University of Oxford working on the synthesis and supramolecular encapsulation of cyclocarbons.

Steffen L. Woltering
Steffen L. Woltering studied Chemistry at the Carl-Georg-August University Göttingen and the University of Edinburgh and obtained his MSc from the former in 2012. He then joined Prof. David Leigh's group in Manchester University and obtained his PhD on the synthesis of interlocked molecules in 2017. Since 2017 he has been carrying out postdoctoral work on carbon-rich systems in the group of Prof. Harry Anderson and on molecular transistors in the group of Prof. Andrew Briggs at the University of Oxford, Department of Materials.

Abstract

The cyclocarbons constitute a family of molecular carbon allotropes consisting of rings of two-coordinate atoms. Their high reactivities make them difficult to study, but there has been much progress towards understanding their structures and properties. Here we provide a short account of theoretical and experimental work on these carbon rings, and highlight opportunities for future research in this field.

Keywords: Carbon | Allotrope | Polyyne

1. Introduction

The family of carbon allotropes continues to expand.[1–3] During the last few decades, fullerenes, carbon nanotubes and graphene joined the founding members, diamond and graphite. Putative 2D allotropes, such as graphdiyne,[4] have been convincingly characterized recently, while more than 500 hypothetical carbon allotropes based on infinite 3D networks are waiting to be synthesized.[1,5] The intriguing topologies of some of these imaginary lattices, such as the Mackay crystal,[6] are also inspiring the synthesis of new molecular nanocarbons.[7]

Small molecular carbon clusters (C_n, where $n = 2$–60)[8] have been detected in comets, sunspots, stars and interstellar clouds.[9] They also have important roles in flames and as intermediates in the plasmas used to produce thin films of diamond.[8] Carbon clusters have been studied in the gas phase since early in the 20th century,[10] and the astrophysical importance of the C_2 molecule was recognized in the 1930s.[11] In 1942, Hahn and co-workers used mass spectrometry to detect carbon ions from C_1^+ to C_{15}^+ in the vapor generated by an electrical discharge between graphite electrodes.[12] Laser vaporization techniques enabled these studies to be extended to cover the whole range of clusters from C_2^+ to beyond C_{600}^+.[13] In 1985, Kroto and co-workers noticed that C_{60} becomes the dominant species when carbon clusters are equilibrated in a helium environment.[14] They conjectured that the C_{60} molecule has an icosahedral "football" geometry, and they named it 'buckminsterfullerene' after the architect of geodesic domes, Buckminster Fuller. Although this structural assignment was speculative, it was confirmed five years later when Krätschmer and co-workers isolated solid C_{60}, initiating the field of fullerene chemistry.[15]

Cyclocarbons are molecular carbon allotropes consisting of rings of two-coordinate *sp*-hybridized carbon atoms. Early studies of carbon clusters provided no information on the molecular geometry, and it was generally assumed that the clusters had linear polyyne or cumulene structures.[8] However, theoretical work indicated that the most stable shapes of C_n clusters evolve from linear chains (when n is small) to rings (for intermediate n) to polycyclic cages (when n is large), as illustrated schematically in Figure 1. Strong experimental evidence for cyclic structures emerged during the 1980s from gas-phase reactivity studies,[16] UV photoelectron spectroscopy[17] and ion mobility measurements.[18] Diederich's first rational synthesis of C_{18}, which was published in 1989, a year before the isolation of C_{60}, aroused further excitement.[19] Despite the apparent simplicity of cyclocarbon molecules, theoretical predictions about their structures have often been contradictory and controversial. Some of this uncertainty was removed by the recent imaging of C_{18} by atomic force microscopy (AFM),[20,21] which revealed a polyynic structure, but many features of these molecules are still poorly understood. Here we provide a concise overview of theoretical and experimental work on these cyclic molecular carbon allotropes.[22]

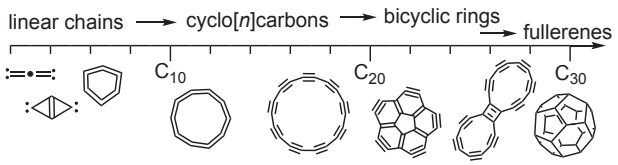

Figure 1. Structural evolution of carbon clusters with increasing size.

In any field of research, people tend to assume (often incorrectly) that all the great discoveries have already been made. During the late 1980s (when the first author of this article was studying for his PhD), it was generally assumed that all carbon clusters are exotic gas-phase species that could never be isolated as pure materials. At that time, it seemed inconceivable that a new soluble carbon allotrope would soon be prepared in bulk, as a stable crystalline solid, just by subliming graphite in helium. Perhaps, in the not too distant future, we will discover a way to tame cyclocarbons by supramolecular encapsulation, so that they become stable under ambient conditions, making it easier to exploit their unusual properties. Even if cyclocarbons cannot be isolated in bulk, they have great potential as precursors to other carbon-rich materials. For example, they appear to be key intermediates in the formation of fullerenes from graphite vapor,[23–25] and they may be precursors to infinite carbon lattices such as graphyne and graphdiyne.[3]

2. Theoretical Studies of Cyclo[*n*]carbons

2.1 Thermodynamic Stability: *Linear vs. Ring vs. Cage.* To the best of our knowledge, the first publication to discuss cyclocarbons is a report by Pitzer and Clementi from 1959.[26] Although this article does not use the word "aromaticity", it correctly predicts that cyclic C_n molecules where $n = 4k + 2$ (with k being an integer) are particularly stable, and it states: *'The pattern of ring orbitals is repeated for the $2p_\pi$ orbitals perpendicular to the plane and for those radially oriented in the plane of the ring'*. This is essentially the principle of double aromaticity (Figure 2), which was first proposed by Schleyer 20 years later,[27] first applied to cyclocarbons by Diederich and co-workers,[19] and subsequently developed by Fowler.[28] In 1966, Hoffmann reported extended Hückel calculations on linear and cyclic C_n for $n = 4$–18 and concluded that rings are more stable than linear chains for C_{10}, C_{14} and C_{18}.[29] These conclusions were confirmed by higher levels of theory, for example Figure 3 shows a plot of the relative stability of rings *vs.* linear chains from DFT calculations, predicting that rings are more stable than linear chains when $n \geq 10$.[30] Recent computational studies give a similar picture, although the question of whether C_6 and C_8 are more stable in cyclic geometries continues to be debated.[31–34] The transition from a monocyclic to bicyclic/polycyclic/cage structures appears to occur at around C_{20} (Figure 1),[35,36] which is the smallest carbon cluster capable of adopting a fullerene structure, with twelve

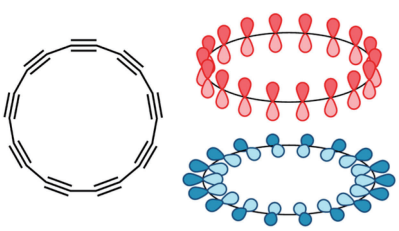

Figure 2. Cyclo[*n*]carbons where $n = 4k + 2$ (with k being an integer) are expected to be doubly aromatic because the two perpendicular sets of p-orbitals each form an aromatic system, as illustrated here for C_{18}.

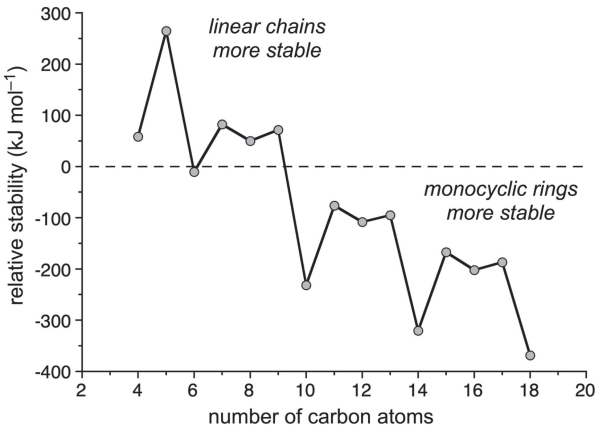

Figure 3. Relative stability of linear versus monocyclic isomers for C_n, where $n = 4$–18 from DFT calculations. Data from ref. 30.

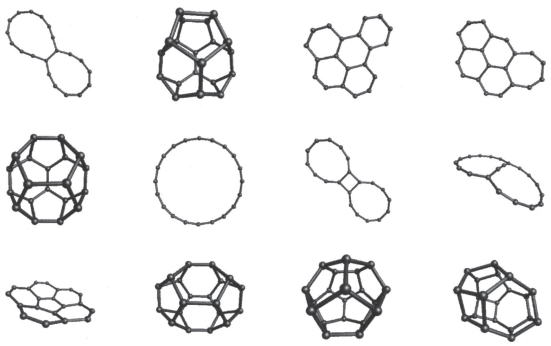

Figure 4. Some low-energy isomers of C_{20} from DFT calculations. Modified from ref. 36 with the permission of AIP Publishing.

pentagons.[37,38] There are many isomers of C_{20} with comparable stability (Figure 4),[36,39] and recent calculations indicate that the corannulene-like structure (bottom left in Figure 4) is lowest in energy.[40]

2.2 Molecular Geometry: *Bond Length Alternation vs. Bond Angle Alternation.* Bond length alternation (BLA) is a fundamentally important parameter when describing π-conjugated molecules, and high levels of BLA indicate weak conjugation.[41] Lack of BLA is a characteristic signature of aromatic molecules such as benzene, so doubly aromatic C_n molecules (with $n = 4k + 2$) might be expected to adopt regular cumulenic D_{nh} geometries, with n C=C bonds (BLA = 0). In contrast, Jahn-Teller distortions in antiaromatic C_n molecules, with $n = 4k$, would be expected to cause BLA, resulting in alternating C-C single and C≡C triple bonds, giving a polyynic $D_{(n/2)h}$ geometry.[42] Peierls distortions in large C_n molecules would also be expected to favor polyynic $D_{(n/2)h}$ geometries with high BLA, even when $n = 4k + 2$.[43] This preference for a polyynic structure relates to the fact that polyynes are generally more stable than cumulenes.[44] These simple principles provide some guidance, but the situation is more complicated and bond angle alternation (BAA) frequently arises, particularly in small cyclocarbons, as illustrated for C_4–C_{10} in Figure 5.[45]

Four types of geometries must be considered for cyclo[n]carbons when n is an even number (as illustrated for C_{18} in Figure 6): **A** D_{nh} cumulene (BLA = 0; BAA = 0), **B** $D_{(n/2)h}$ polyyne (BLA ≠ 0; BAA = 0), **C** $D_{(n/2)h}$ cumulene (BLA = 0; BAA ≠ 0) and **D** $C_{(n/2)h}$ polyyne (BLA ≠ 0; BAA ≠ 0).

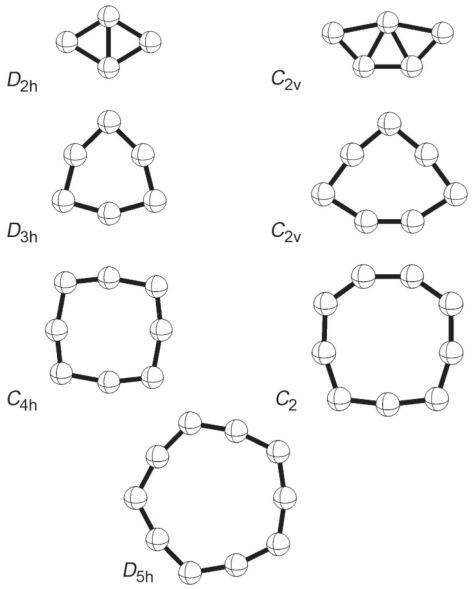

Figure 5. Structures for the neutral cyclic carbon clusters C_4–C_{10} calculated at CCSD(T) level of theory.[45] All the geometries are planar, except C_9. Modified with permission from ref. 45. Copyright 2007 American Chemical Society.

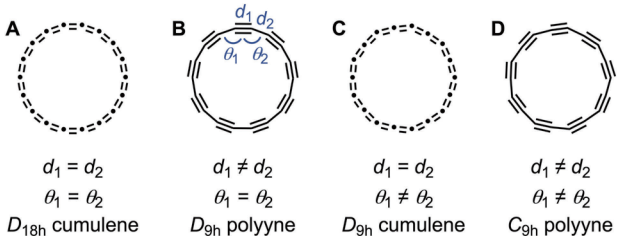

Figure 6. Four possible structures of a cyclo[n]carbon, when n is an even number, illustrated for C_{18}. The bond length alternation is defined as BLA = $d_1 - d_2$ and the bond angle alternation is defined as BAA = $\theta_1 - \theta_2$.

The predictions of the lowest energy geometry **A**–**D** for C_n, where $n = 6$–24, from many computational studies are summarized in Table 1.[19,28,30,33,38,42,43,45–58] This survey points to the following three generalizations:

- Small aromatic rings ($n = 4k + 2$) with $n \leq 10$ have structure **C** (BLA = 0; BAA ≠ 0).
- Small antiaromatic rings ($n = 4k$) with $n \leq 16$ have structure **D** (BLA ≠ 0; BAA ≠ 0).
- Large rings ($n \geq 24$) have polyyne structures **D** or **B** (BLA ≠ 0).

The structures of intermediate rings ($16 < n < 24$) are difficult to calculate and the results are highly dependent on the computational method. For example, most density functional theory (DFT) and second-order Møller-Plesset (MP2) calculations predict that the lowest-energy geometry of C_{18} is cumulenic (**A** or **C**), whereas Hartree-Fock (HF), quantum Monte Carlo (MC) and coupled cluster methods predict that the polyyne form is the ground state (**B** or **D**). Hybrid-DFT

Table 1. Survey of the predicted ground state geometries of even cyclo[*n*]carbons C_6–C_{24}.[a]

year [ref.]	C_6	C_8	C_{10}	C_{12}	C_{14}	C_{16}	C_{18}	C_{20}	C_{22}	C_{24}	level of theory
1986 [46]	**C**										HF
1989 [19]							**B**				HF
1990 [47]			**C**								CISD/DZP
1991 [48]							**B** **A**				SCF MP2
1992 [49]			**C**								SCF and CCSD/cc-pVDZ
1992 [38]							**B** **A**	**B** **B**	 **A**	**B** **B**	SCF MP2
1994 [30]	**C**		**C**	**D**	**A**	**D***	**A***				DFT (* not energy minima)
1995 [50]			**C** **C**		**C** **D**		**C** **D**				DFT/6-31G*/B-LYP RHF/6-31G*
1995 [51]	**C**	**D**	**C**	**D**	**C**	**D**	**C**				DFT/cc-pVDZ/B3LYP
1999 [42]	**C**		**C**		**C**		**C**		**D**		DFT/cc-pVDZ/B3LYP
2000 [43]	**C**	**D**	**C**	**D**	**C**	**D**	**C**	**B**	**C**		LDA/84Ry
2000 [52]	**C**		**C**		**B**		**B**				QMC
2005 [53]							**C**		**C**		DFT/6-31G*/B3LYP
2007 [45]	**C**	**D**	**C**								CCSD(T) cc-pVTZ
2008 [54]	**C**		**C**		**D**		**D**		**D**		CCSD cc-pVTZ
2009 [28]	**C**	**D**	**C**	**D**	**C**	**D**	**C**	**D**	**C**	**D**	DFT/6-31G(d)/B3LYP
2010 [55]			**C**		**B**		**B**		**B**		DFT/cc-pVDZ/rCAM-B3LYP
2016 [33]	**C**	**D**	**C**	**D**	**C**	**D**	**C**	**D**	**C**	**D**	DFT/6-311++g(d,p)/*meta*-GGA
2019 [56]							**B**				DFT/def2-TZVP/RSX-PBE
2019 [57]							**B**				CASSCF
2020 [58]	**C**	**D**	**C**	**D**	**D**	**D**	**D**	**D**	**D**	**D**	DFT/6-311++G(d,p)/ωB97XD

[a]See Figure 6 for definition of structural types **A**–**D**. Abbreviations: HF: Hartree-Fock; CISD: configuration interaction with single and double excitations; DZP: *d* polarization functions; SCF: self-consistent field; MP2: second-order Møller-Plesset; CCSD: coupled-cluster singles and doubles; cc-pVDZ: Dunning's correlation consistent polarized valence double-zeta basis set. 6-31G*: a Pople basis set; B-LYP and B3LYP: Beck-Lee-Yang-Parr functionals; LDA: local-density approximation; QMC: quantum Monte Carlo; CASSCF: complete active space SCF method; RSX-PBE: range-separated exchange Perdew-Burke-Ernzerhof functional; def2-TZVP: Ahlrichs et al. triple zeta valence polarization basis set; ωB97XD: a long-range corrected hybrid density functional.

functionals (such as rCAM-B3LYP, RSX-PBE and ωB97XD) that include enough exchange correlation also correctly predict a polyyne structure for the larger rings.[55,56,58]

The crossover from BAA to BLA in the size range $n = 6$–26 is illustrated for aromatic rings ($n = 4k + 2$) in Figure 7, by comparing results from a range of theoretical methods.[43,52,54,58] Different levels of theory agree in predicting a decline in BAA from about 55° in C_6 to <5° in C_{22}, and many of them predict an increase in BLA from 0 in C_6 and C_{10} to about 0.1 Å in C_{22}, however predictions diverge in the intermediate size regime (particularly for C_{14} and C_{18}).

At first sight, BAA looks strange and counter-intuitive, as it contradicts expectations from valence-shell electron-pair repulsion theory, so it is worth considering why it arises. The Walsh diagram for C_6 (Figure 8a) shows that all the π-orbitals decrease in energy as the molecule distorts from D_{6h} to D_{3h}.[59,60] In the D_{6h} geometry, the in-plane *p*-orbitals create a high electron density at the center of the molecule, which destabilizes the structure. Distortion to D_{3h} symmetry shifts electron density towards the edges of the molecule, resulting in a lower energy. This distortion changes the hybridization of alternating atoms to sp^2, and these sp^2 centers have partial negative charge while the remaining *sp* centers are positively charged (Figure 8b).[33]

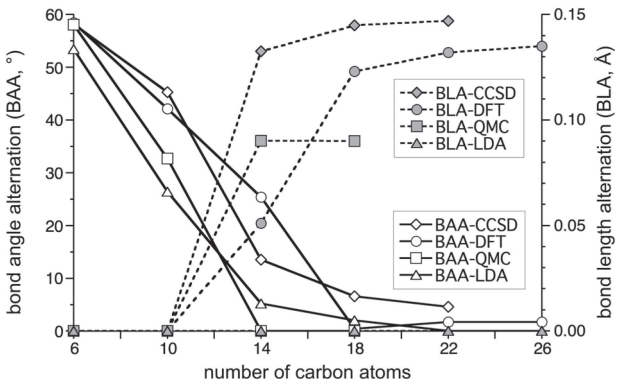

Figure 7. Evolution of BAA and BLA for even rings C_6–C_{26} predicted from different theoretical methods: CCSD cc-pVTZ (ref. 54); DFT/6-311++G(d,p)/ωB97XD (ref. 58); QMC (ref. 52) and LDA/84Ry (ref. 43).

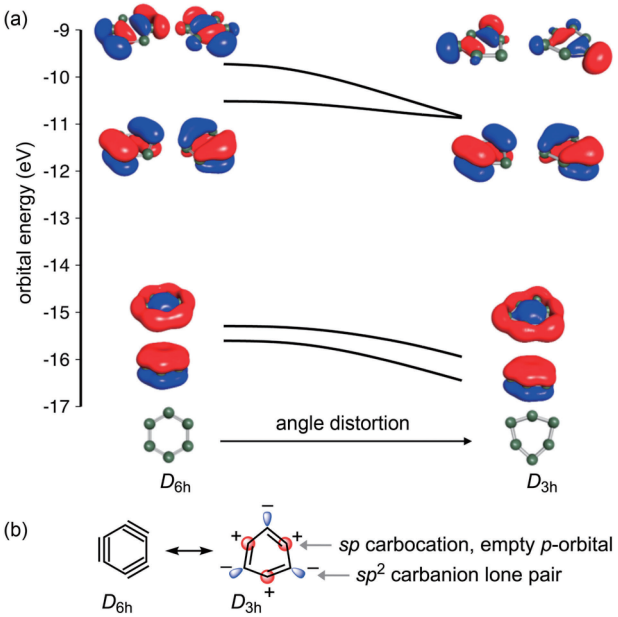

Figure 8. (a) A Walsh diagram showing how the energy of the four highest occupied orbitals of C_6 evolves as the symmetry changes from D_{6h} to D_{3h}.[59,60] (b) A resonance diagram showing how the hybridization and charge distribution changes with increasing BAA.[33]

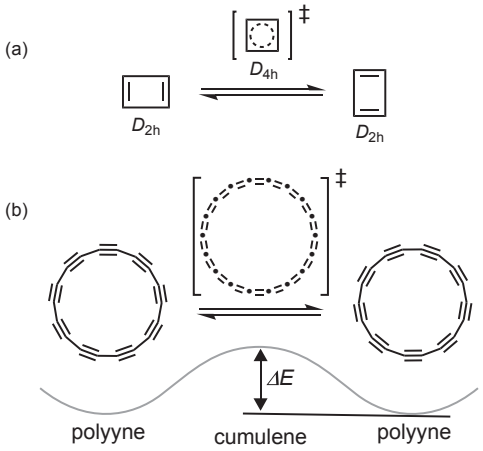

Figure 9. (a) Bond-shift valence tautomerism interconverts the positions of the single and double bonds of cyclobutadiene via a square transition state. (b) A similar process interconverts the single/triple bonds of C_{18}.[57,58,62–64]

The discussion above focused on the molecular geometries of cyclo[*n*]carbons where *n* is an even number. There have also been many theoretical studies of odd cyclocarbons.[28,30,32,34,45,61] In most cases, C_{2v} or C_2 (nonplanar) geometries are predicted, as illustrated by the structures of C_5, C_7 and C_9 in Figure 5.[45]

2.3 Dynamics: *Bond-Shift Valence Tautomerism.* A cyclic molecule with BLA and/or BAA can often shift between low-symmetry geometries via a more symmetrical transition state. This type of rearrangement is known as bond-shift valence tautomerization or automerization, and it can be understood by considering cyclobutadiene, which has a rectangular D_{2h} ground state (Figure 9a). The long and short bonds interchange via a square D_{4h} transition state. Interconversion of the two rectangular forms has a barrier of about 30 kJ mol^{-1} and occurs with a half-life of about 1 ms at 25 K.[62] C_{18} is predicted to undergo bond-shift valence tautomerization via a cumulenic transition state with an energy barrier of about 40 kJ mol^{-1} (Figure 9b).[57,58,63,64] Quantum mechanical tunneling is predicted to accelerate this process and the half-life for interconversion of the two degenerate forms of C_{18} is calculated to be approximately 3 ns at 5 K.[64,65] The rate of valence tautomerism is faster than in cyclobutadiene, despite the higher barrier, because in C_{18} the barrier is narrower (i.e. the distances moved by the atoms are smaller), leading to faster tunneling.

3. Experimental Studies of Cyclo[*n*]carbons

3.1 Carbon Clusters from the Vaporization of Graphite. The high-temperature vaporization of graphite, by laser ablation or other heating methods, generates a broad distribution of carbon clusters, containing both linear and cyclic isomers, often dominated by short linear chains.[8] These mixtures can be analyzed in the gas phase, after mass-selection and even shape-selection, to give information on the molecular geometry and electronic structure. Here we highlight the main experimental techniques that have been used to characterize cyclo[*n*]carbons in the gas phase.

3.1.1 Mass Spectrometry and Magic Numbers: Mass spectra do not normally provide structural information, but they gave the first hint of experimental evidence to confirm the prediction that C_n ions with $n > 9$ are cyclic. Pitzer and Clementi pointed out that 'magic number' cyclic clusters with $n = 4k + 2$ should have greater stability (as mentioned above), which should make them more abundant, leading to peaks in the cluster distribution with a periodicity of $\Delta n = 4$, with the most intense signals at C_{10}, C_{14}, C_{18}, etc.[26] In contrast, the stabilities of linear chains are expected to alternate with increasing length, with a periodicity of $\Delta n = 2$. This switch in periodicity from $\Delta n = 2$ for small clusters to $\Delta n = 4$ for $n \geq 10$ is observed for both C_n^+ and C_n^- ions, and this was taken as evidence for a transition from linear chains to rings.[8,66] But, confusingly, the most abundant species are C_{11}, C_{15}, C_{19}, etc. for positive ions and typically C_{12}, C_{16}, C_{20}, etc. for negative ions, not the expected $n = 4k + 2$ species.[66] Two factors explain this anomaly: (a) changing the charge changes the value of *n* that confers aromatic stability, and the mass distribution equilibrates after ionization, and (b) the pattern of intensities in the mass spectrum reflects the ionization energies, not just the distribution of cluster sizes.[8] If neutral C_n clusters are photoionized to C_n^+ without providing enough energy for fragmentation and re-equilibration of the cluster size distribution, the most intense signals are observed for C_{10}^+, C_{14}^+, C_{18}^+, etc. (as expected from the stabilities of the neutral clusters plotted in Figure 3).[67]

3.1.2 Gas-Phase Reactivity Studies: McElvany and coworkers pioneered the use of Fourier transform ion cyclotron resonance spectrometry to study the reactivity of mass-selected carbon cluster ions (C_n^+; $n = 3$–20) with neutral molecules such as D_2, O_2, CH_4, C_2H_2, C_2H_4 and HCN.[16] A change in reactivity was observed as a function of cluster size, suggesting a structural transition from linear to monocyclic rings at C_{10}^+,

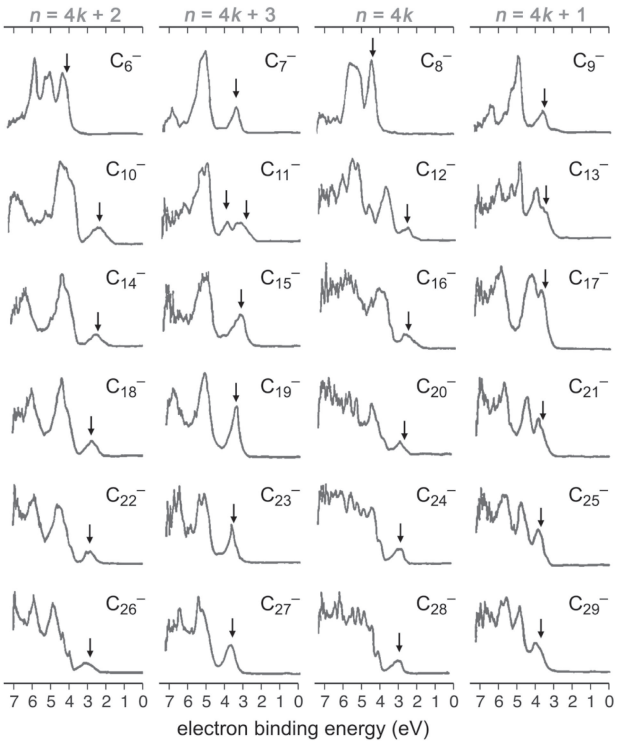

Figure 10. Ultraviolet photoelectron spectra of mass-selected C_n^- anions from C_6^- to C_{29}^-. The vertical arrows indicate the photodetachment thresholds, which were used to estimate the electron affinities of the neutral clusters. Columns show the similarity for ions with $n = 4k + 2$, $n = 4k + 3$, $n = 4k$, and $n = 4k + 1$ where $n \geq 10$. Reprinted with permission from ref. 17. Copyright 1988 Elsevier B.V.

with rings being dramatically less reactive than linear chains. These experiments indicated that C_7^+, C_8^+ and C_9^+ exist as mixtures of linear and cyclic isomers, whereas C_{10}^+ and larger clusters are entirely cyclic.

3.1.3 Gas-Phase Ultraviolet Photoelectron Spectroscopy (UPS): One of the first pieces of experimental evidence for neutral cyclic carbon clusters was provided by Smalley and co-workers in 1988.[17] They determined the electron affinities of the neutral clusters by measuring the UPS spectra of negatively charged C_n^- ions. In this experiment, UV light is used to remove an electron from mass-selected C_n^- anions ($n = 2$–29), and the threshold for electron detachment gives the electron affinity of the neutral cluster. The results (Figures 10 and 11) show an odd-even alternation in the electron affinity, due to the changing electronic structure of the C_n cluster, with an abrupt transition at $n = 10$, due to a change in geometry from linear to cyclic structures. Linear C_n chains with even n have higher electron affinities, due to their open-shell ground states, whereas for the rings, the n-odd species have higher electron affinities. Two electron affinities are measured for C_{11}, due to the presence of both linear and cyclic structural isomers.

The shapes of the UPS spectra provide information on the electronic structure, as seen in Figure 10. There is a close resemblance between the spectra of the C_n^- anions where $n = 4k + 2$ (i.e. C_{10}, C_{14}, C_{18}, C_{22} and C_{26}), reflecting the Hückel aromatic structures of the corresponding neutral C_n species.

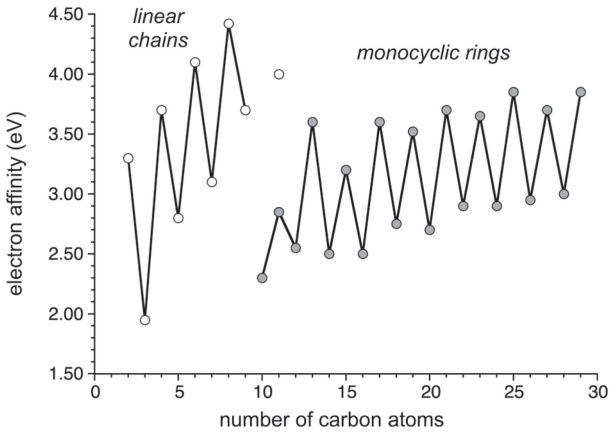

Figure 11. Plot of electron affinities (from the UPS spectra in Figure 10) against the number of carbon atoms for C_2 to C_{29}. Data from ref. 17.

Similarly, characteristic UPS spectra are observed for the $n = 4k$, $n = 4k + 1$ and $n = 4k + 3$ families of C_n^- anions in the range $n = 11$–29.

3.1.4 Gas-Phase Ion Chromatography: This technique allows isomeric molecular ions to be separated by shape. A pulse of mass-selected ions is injected into a cell filled with helium and the ions drift through the cell under the influence of a weak electric field. Compact ions, such as those with ring structures, are more mobile than linear ions, because they make fewer collisions with helium atoms, so they arrive earlier at the detector. This technique was first applied to carbon clusters by Bowers and co-workers in the early 1990s.[18,25,68,69] For example, Figure 12 shows the mobility results for positively charged carbon clusters of up to C_{60}^+.[18] Cycloalkanes and linear alkenes were used as references to distinguish between different structures. It was found that different isomeric species coexist for many cluster sizes. For up to 10 carbon atoms, linear and cyclic clusters are observed, but only monocyclic rings are detected in the range C_{10}^+ to C_{20}^+. From C_{21}^+ onwards, an additional type of species of higher mobility is observed, which appears to be bicyclic rings (Figure 12a). From 30 carbon atoms onwards, even more species are observed, including three-dimensional fullerenes. No monocyclic carbon clusters are observed beyond C_{36}^+. Similar results were achieved for negatively charged carbon clusters,[68] although linear configurations are observed up to C_{20} for anionic species, and the charge state evidently affects the relative stability of rings *vs.* linear chains. Ion chromatography has also been used to monitor the gas-phase rearrangement and fragmentation of cyclo[n]carbon cations,[25,69] and the reaction of cyclo[n]carbon cations with neutral molecules such as D_2.[70]

3.1.5 Gas-Phase Electronic Spectroscopy: The absorption spectra of carbon clusters have attracted interest because they could potentially be used to identify these species in diffuse interstellar bands (wavelength: 440–900 nm; frequency: 11,000–23,000 cm^{-1}).[9] Maier and co-workers developed a technique for recording mass-selective gas-phase excitation spectra of neutral carbon clusters using resonant two-color two-photon ionization (R2C2PI) spectroscopy.[53] In this experiment, the neutral molecules are excited to higher electronic states

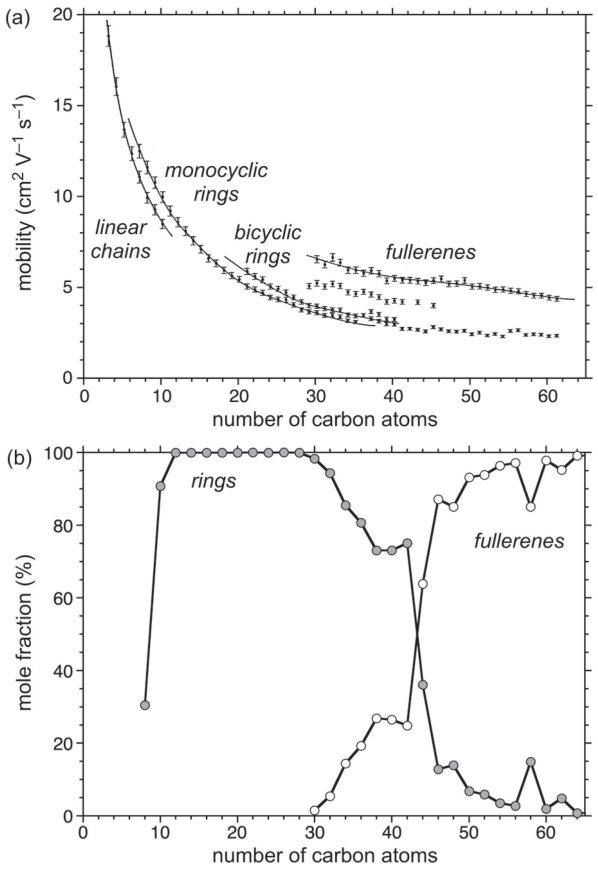

Figure 12. (a) A plot of mobility *vs.* cluster size for positively charged cluster ions C_3^+ to C_{62}^+. Modified from ref. 18 with the permission of AIP Publishing. (b) Plot of the mole fraction of planar rings (monocyclic and bicyclic) and fullerenes for C_n^+ cluster cations where n is even. Data from ref. 25.

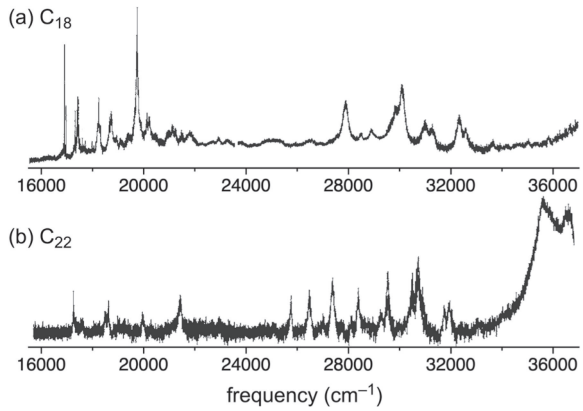

Figure 13. Gas-phase electronic ultraviolet-visible spectra of (a) C_{18} and (b) C_{22} recorded by R2C2PI. Modified from ref. 53 with the permission of AIP Publishing.

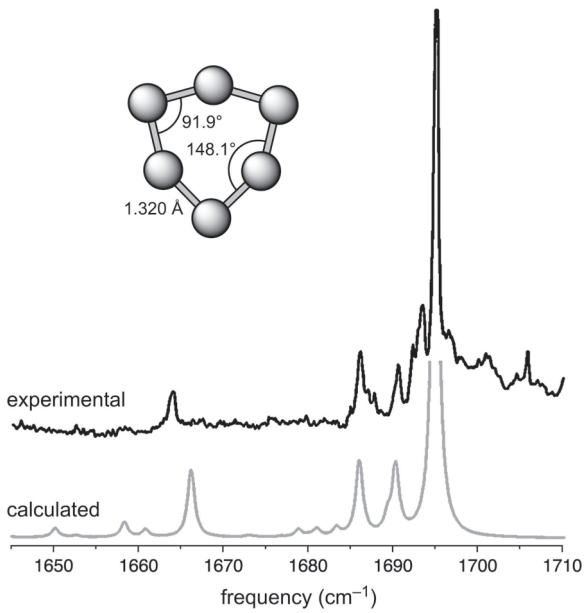

Figure 14. Experimental (top) and calculated (bottom) IR spectrum of C_6 recorded in solid argon at 10 K. The simulated spectrum is based on the predictions of the B3LYP/cc-pVTZ DFT calculations, which give the ground-state D_{3h} geometry illustrated. Modified from ref. 75 with the permission of AIP Publishing.

with one laser and then ionized with a second laser; the ionized molecules are then detected and analyzed in a mass spectrometer. The ion current is monitored as the wavelength of the first laser is scanned to record an absorption spectrum. If light from the first laser is not absorbed, the second laser does not provide sufficient energy to ionize the molecule.

The UV-visible spectra of cyclic C_{18} and C_{22}, measured by R2C2PI, are shown in Figure 13.[53] The similarity between these spectra reflects their homologous Hückel-aromatic $4n + 2$ structures. The vibronic transitions were compared with calculated spectra to gain insights into the structures of these clusters. The number of observed transitions indicates that the molecules adopt low-symmetry polyyne geometries: D_{9h} or C_{9h} for C_{18} and D_{11h} for C_{22}, rather than cumulenic D_{18h} and D_{22h}, respectively (i.e. **B** or **D** in Figure 6, rather than **A** or **C**). The electronic spectrum of C_{14}, measured by the same method, consists of sharper lines over a narrower range (19,000–20,000 cm^{-1}), compared with the spectra of C_{18} and C_{22}, indicating that C_{14} has a more symmetrical cumulene geometry (**A** or **C** in Figure 6).[71]

3.1.6 Matrix Isolation: It is difficult to study carbon clusters in the gas phase because they can only be prepared at low concentrations. Consequently, there have been many studies in which carbon clusters, from the vaporization of graphite, have been condensed into inert gas matrices (solid Ne, Ar or N_2) and studied at low temperatures.[72] The first cyclo[*n*]carbon to be convincingly identified in this way was cyclic C_6.[73–75] The IR spectrum of this cluster in argon at 10 K matches extremely well with the calculated spectrum for D_{3h} C_6 (from CCSD(T) and B3LYP/cc-pVTZ DFT calculations) as shown in Figure 14.[74,75] This structural assignment was confirmed by the good match with theoretically predicted ^{13}C isotopic shifts. IR peaks due to cyclic C_8 with C_{4h} symmetry were also detected under the same conditions.[76,77] In these experiments, C_6 and C_8 were not mass-selected; instead, they were formed in the argon matrix from the reaction of smaller carbon clusters such as C_2 and C_3 during annealing at around 30 K. This reaction gives mainly cyclo-C_6.

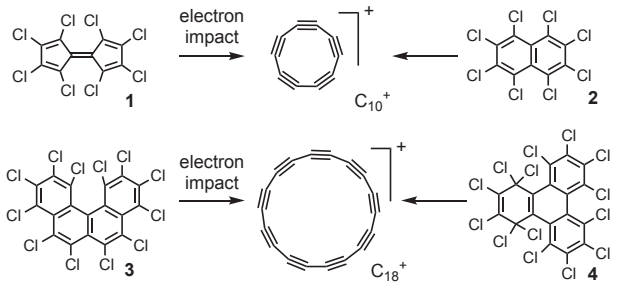

Figure 15. Formation of C_{10}^+ and C_{18}^+ by gas-phase electron-impact ionization on chlorocarbon precursors.[80]

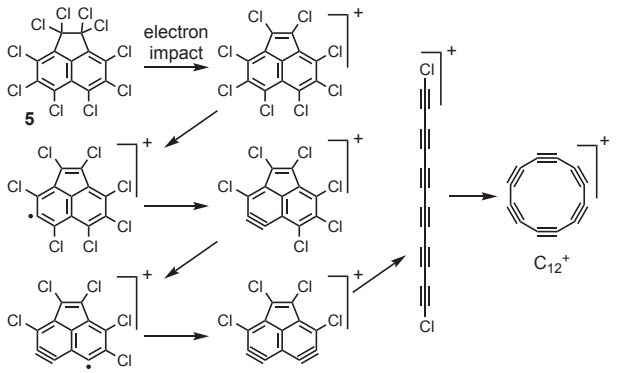

Figure 16. The pathway for formation of C_{12}^+ from **5** deduced from ion mobility measurements.[81]

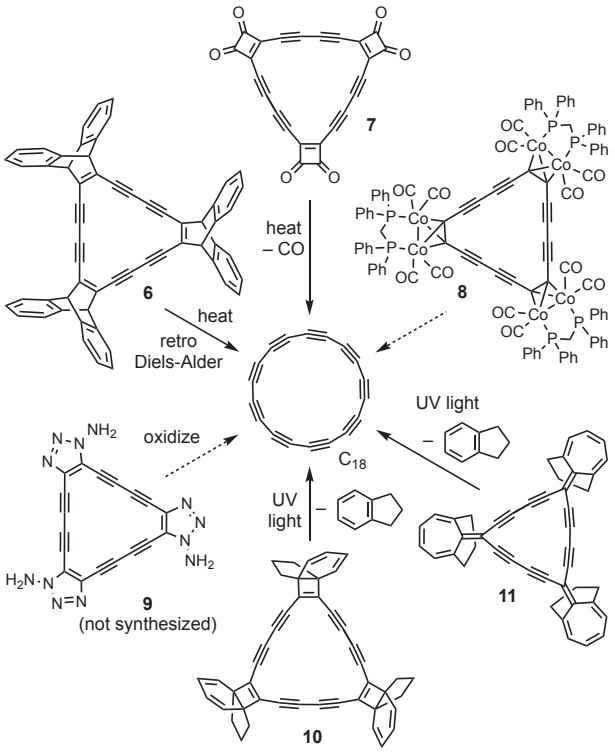

Figure 17. Potential routes to C_{18} from molecular precursors.

Surface-enhanced Raman spectra of mass-selected C_{14}, C_{16}, C_{18} and C_{20} clusters in a matrix of solid N_2 at 10 K gave spectra that were most consistent with linear chain isomers, perhaps due to rearrangement of ring isomers during deposition from the gas phase into the matrix.[78] The electronic (UV-visible) spectra of mass-selected cyclic C_{10}, C_{12} and C_{14} in neon at 6 K have also been reported.[79]

3.2 Carbon Clusters from the Molecular Precursors. 3.2.1 From Halocarbons by Electron Impact: Lifshitz and co-workers demonstrated that cationic carbon clusters, C_n^+ ($n = 3$–20), can be generated from a wide variety of chlorocarbons C_nCl_x by gas-phase electron impact ionization and successive loss of chlorine atoms, as illustrated in Figures 15 and 16.[80] The structure of the chlorocarbon does not seem to matter in these experiments, and both isomers of $C_{10}Cl_8$ (compounds **1** and **2**) gave C_{10}^+ with the same gas-phase reactivity, while precursors **3** and **4** ($C_{18}Cl_{12}$ and $C_{18}Cl_{14}$, respectively) both gave C_{18}^+. The reactivities of these C_n^+ cations indicate that they are cyclic for $n \geq 10$ and their gas-phase properties are identical to those of C_n^+ cations generated from vaporization of graphite.[80] Ion chromatography has been used to analyze the intermediates in the conversion of $C_{12}Cl_{10}$ (**5**) to C_{12}^+ (Figure 16).[81] The framework of the molecule remains predominantly intact while the first six chlorine atoms are removed, then upon removal of two more chlorines, the molecule springs open to form a linear $C_{12}Cl_2^+$ chain, then it closes to a monocyclic ring when the final chlorine atoms are lost.

The C_6^+ cation generated from gas-phase electron impact ionization of hexachlorobenzene (C_6Cl_6) and hexabromobenzene (C_6Br_6), have been condensed in a neon matrix and studied by IR and electronic spectroscopy at 6 K.[82] C_6Br_6 was found to generate mainly cyclic C_6^+ whereas C_6Cl_6 gave a mixture of linear and cyclic isomers. Similar gas-phase debromination reactions were used to synthesize the smallest fullerene C_{20} from $C_{20}HBr_{13}$ (prepared by solution-phase bromination of dodecahedrane, $C_{20}H_{20}$).[37]

3.2.2 Organic Synthetic Approaches to C_{18}: The challenge of preparing cyclocarbons by rational total synthesis was first addressed by Diederich in 1989.[19,23,83,84] These efforts focused on C_{18} because of its anticipated stability and synthetic accessibility. Diederich's group (particularly Rubin) explored three types of reactions for unmasking C_{18} in the final step of the synthesis: retro Diels-Alder reactions from compound **6**,[19] decarbonylation of carbon oxide **7**,[23,85,86] and decomplexation of cobalt from compound **8**,[87] as summarized in Figure 17. All three of the precursor compounds **6**–**8** were thoroughly characterized, including by single-crystal X-ray crystallography. Larger homologues of these macrocycles were also studied as precursors of C_{24} and C_{30}.

Laser flash heating of **6** resulted in a three-fold retro Diels-Alder reaction generating C_{18}, as detected by two-photon ionization mass spectrometry (Figure 18).[19] The authors proposed that flash vacuum pyrolysis[88] of **6** could provide a route to the bulk preparation of C_{18}, but this reaction only yielded anthracene and polymeric material. Laser desorption mass spectra of carbon oxide **7** reveal the successive loss of CO molecules to give C_{18}, in both positive and negative modes.[86] Larger homologues of **7** generated C_{24} and C_{30} under the same conditions, and these mass spectra provided insights into the mechanism of fullerene formation.[23,24] It was found that C_{30}^+ coalesces selec-

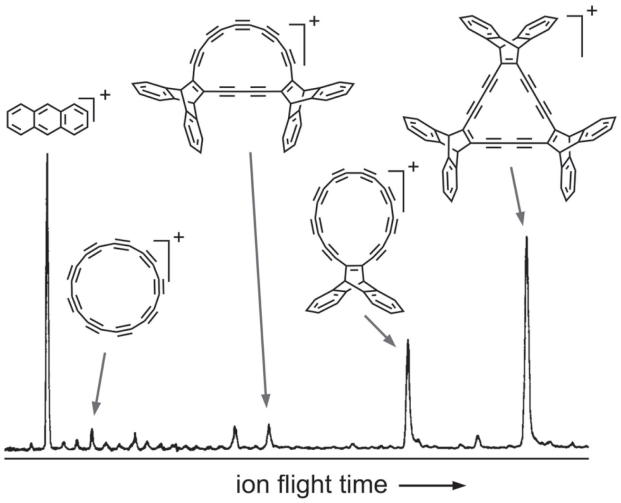

Figure 18. Time-of-flight mass spectra of compound **6** showing products from the loss of anthracene via retro Diels-Alder reactions. Modified from ref. 19. Reprinted with permission from AAAS.

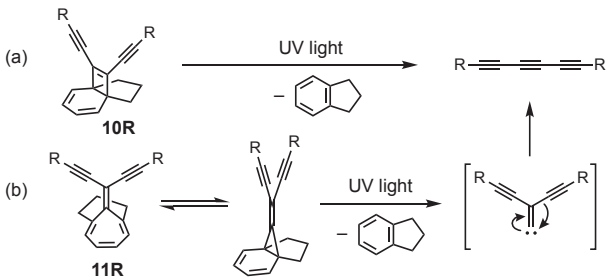

Figure 19. Photochemical unmasking of model compounds: (a) [4.3.2]propella-1,3,11-triene **10R**; yields for this reaction are 66–70%,[92,94] and (b) bicyclo-[4.3.1]deca-1,3,5-triene **11R**; yields for this reaction are 43–47% depending on the R group.[93,95]

tively into C_{60}^+, whereas C_{18}^+ and C_{24}^+ form mainly C_{70}^+. Previously, it was thought that fullerenes were formed directly from small carbon fragments, such as C_2, upon vaporization of graphite.[89] This result indicates that cyclocarbons are intermediates in the conversion of C_2 to C_{60} and C_{70}. Irradiation of **7** in a matrix of solid 1,2-dichloroethane at 15 K was monitored by IR spectroscopy, showing the release of CO, but no spectroscopic signature of C_{18} was detected.[84]

The cobalt complex **8** is a fascinating structure, as a metal complex of C_{18}, but all attempts at removing the cobalt were unsuccessful.[84,87] Another potential route to C_{18}, from compound **9** involves oxidation of a 1-amino-1,2,3-triazole.[90] This type of reaction is effective for the generation of benzynes,[91] but the attempted synthesis of compound **9** was unsuccessful and this route has not been fully tested.

Tobe made major contributions to the rational synthesis of cyclocarbons by developing masked alkyne equivalents (MAEs) that can be unmasked photochemically, as applied in precursors **10** and **11**.[92,93] These MAEs form alkynes by eliminating indane upon UV irradiation, as illustrated for the photolysis of model compounds **10R** and **11R** in Figure 19.[92–95] Both **10** and **11** are converted into C_{18}^- during negative-mode

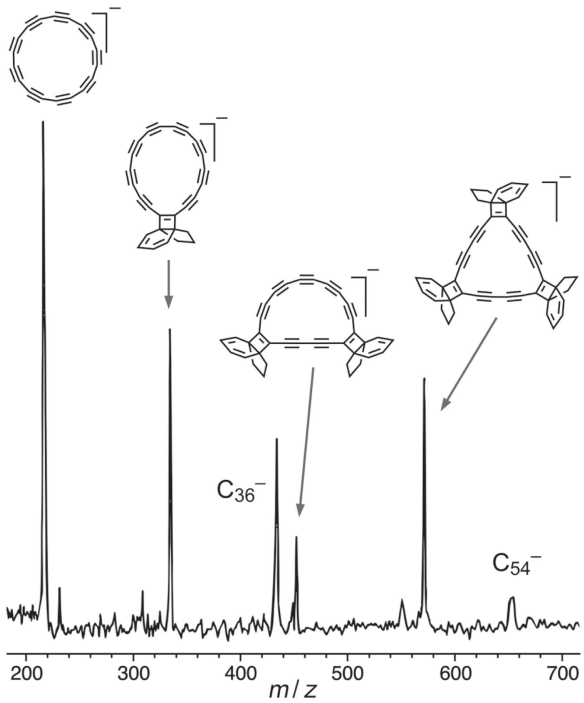

Figure 20. Negative ion laser-desorption time-of-flight mass spectrum of compound **10** showing the elimination of indane to form C_{18}. Adapted with permission from ref. 92c. Copyright 1996 American Chemical Society.

time-of-flight laser-desorption mass spectrometry, as illustrated for **10** in Figure 20. The structures of the carbon cluster anions (C_{12}^-, C_{16}^-, C_{18}^-, C_{20}^- and C_{24}^-) generated from **10** and analogous precursors were investigated by UPS, and compared with mass-selected anions generated by laser vaporization of graphite.[96] On the basis of the splitting frequencies due to vibrational excitation of the neutral cyclocarbons produced by detaching an electron from the corresponding anions, it was deduced that cyclo[*n*]carbons with $n = 4k$ (C_{16}, C_{20}, and C_{24}) have polyynic structures with alternating single and triple bonds, and that C_{18} has a cumulenic structure.[96] It was not possible to prepare C_{18} in solution due to its high reactivity, but irradiation of **10** in furan generated **12**, **13** and **14** in which one, two, or all indane units are replaced by the furan moieties, respectively (Figure 21). These results do not imply the direct formation of C_{18} by the photolysis of **10**, but they show that the elimination of at least one of the indane units takes place efficiently by [2 + 2] cycloreversion from **10** (as well as **12** and **13**) to produce highly reactive dehydro[18]annulene intermediates.

One general conclusion from the work summarized in this section is that cyclo[*n*]carbons can be generated selectively from well-designed precursors, but that they are too reactive to be isolated under normal ambient laboratory conditions.

3.2.3 On-Surface Synthesis and Imaging: Scanning probe microscopies (such as atomic force microscopy, AFM, and scanning tunnelling microscopy) are powerful techniques for studying highly reactive molecules such as arynes[97] or radicals[98] on surfaces at low temperature. Tip functionalization techniques, in which the tip is functionalized with species such as carbon monoxide, enable molecules to be imaged with

atomic resolution by AFM.[99] The tip can also be used to move molecules across the surface, and to apply voltage pulses to trigger chemical reactions, in a process known as atom manipulation.[97–102] Gawel, Gross, Anderson and co-workers applied these techniques to re-investigate the formation of C_{18} from compound **7** ($C_{24}O_6$).[20] The cyclocarbon oxide was sublimed onto a bilayer of NaCl on Cu(111) at 5 K and imaged by AFM to view its triangular geometry (Figure 22). Application of a voltage pulse resulted in elimination of carbon monoxide, forming the cyclocarbon. The AFM image of C_{18} exhibits nine bright lobes, indicating that it has a polyynic structure with alternating single and triple bonds. A similar technique was also used to generate C_{18} from bromocyclocarbon **15** ($C_{18}Br_6$), which gave a higher yield of C_{18} and enabled clearer images of C_{18} to be recorded, compared with synthesis from **7**.[21] Experimental images, recorded at a range of tip heights, were compared with simulated images for four model structures (**A**–**D** in Figure 6). This analysis showed that cumulenic D_{18h} (**A**) and D_{9h} (**C**) geometries are not consistent with the observed images, however the simulated images for D_{9h} (**B**) and C_{9h} (**D**) polyynic geometries could not be distinguished. These polyynic geometries, which differ only in that **D** has BAA, give very similar simulated images because the AFM contrast is dominated by the difference in electron density between triple and single bonds. The bright contrast in the AFM image of C_{18} in Figure 22 is observed above the triple bonds. BAA affects the position and orientation of the bonds, without causing large changes in the electron density, resulting in subtle contrast modulations. It is particularly difficult to distinguish between D_{9h} and C_{9h} polyynic geometries for C_{18} because the level of BAA in the C_{9h} geometry is expected to be low (<7° in Figure 7); as the BAA tends to zero, D_{9h} and C_{9h} geometries become identical.

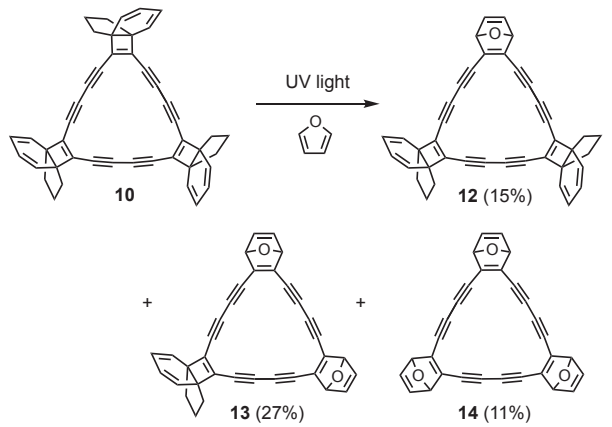

Figure 21. Photolysis of compound **10** as a solution in furan, with a low-pressure mercury lamp.[92] (All four compounds are mixtures of diastereomers.)

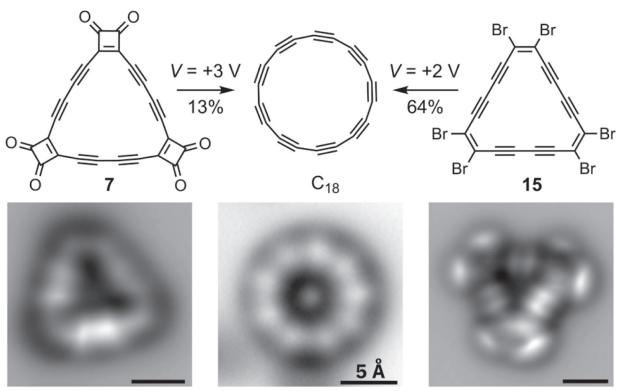

Figure 22. Two routes for generating C_{18} on a NaCl bilayer on a Cu(111) surface at 5 K.[20,21] The experimental AFM images recorded with a CO-functionalized tip are shown below each structure. The central image is of C_{18} prepared from **15**. All three scale bars are 5 Å.

It is surprising that the alternating single and triple bonds in C_{18} can be observed by AFM, considering the prediction that bond-shift valence tautomerism should occur on a time-scale of about 3 ns at 5 K (as discussed above in Section 2.3)[64,65] and that the time-scale of AFM is several seconds. This result implies that quantum mechanical tunneling accelerates this process less than predicted, or that the barrier is higher than expected, or that the interaction with the NaCl surface dramatically retards bond-shift valence tautomerism.

4. Conclusions, Vision and Outlook

The structural characterization of C_{18} by AFM (discussed in the previous section) opens the way for imaging other cyclo[*n*]-carbons. It will be interesting to compare the structures of antiaromatic rings such as C_{16} and C_{20} (with $n = 4k$) and odd-atom rings, such as C_{17} and C_{15}. It will also be fascinating to study small rings such as C_{10}, which are expected to have high levels of BAA (26–45° for C_{10} in Figure 7, compared with 0–7° for C_{18}). Zhao and co-workers have predicted that cyclic C_{10} and C_{14} should be more stable than C_{18}, both kinetically and thermodynamically, suggesting that they are realistic targets for experimental work.[103] Large rings such as C_{20} and C_{24} are also intriguing because they may adopt bicyclic or polycyclic isomers, as illustrated by the many low-energy isomers of C_{20} (Figure 4). The on-surface synthesis of C_{18} from bromocyclocarbon **15** poses the question of whether chlorocarbons such as **3** and **4** (Figure 15) can also be used as precursors for on-surface synthesis of C_{18}.

Diederich proposed that cyclocarbons could be used as precursors to infinite carbon networks such as graphdiyne (Figure 23).[83] The development of better on-surface routes to cyclocarbons may make it possible to realize this idea. Cyclocarbons may also be valuable precursors to amorphous carbon networks, as demonstrated with linear polyynes.[104]

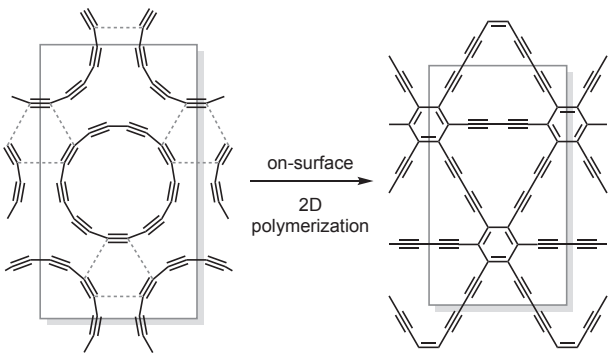

Figure 23. Synthetic approach to the infinite network graphdiyne, proposed by Diederich.[83]

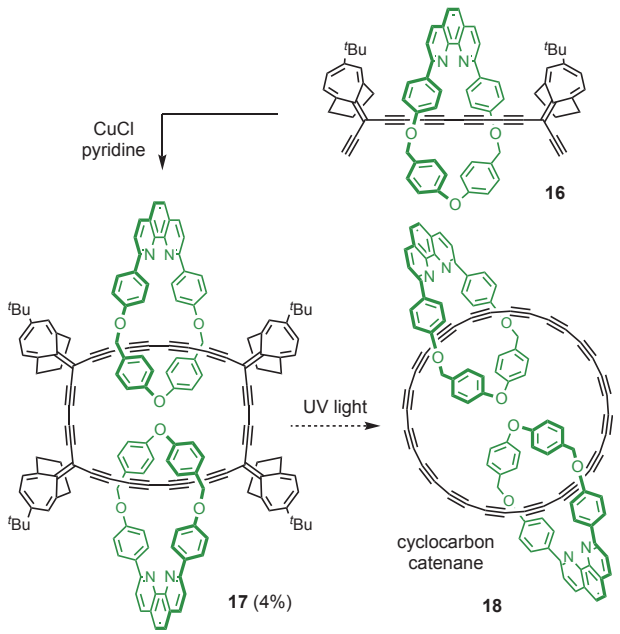

Figure 24. Synthesis of a masked cyclocarbon catenane.[95]

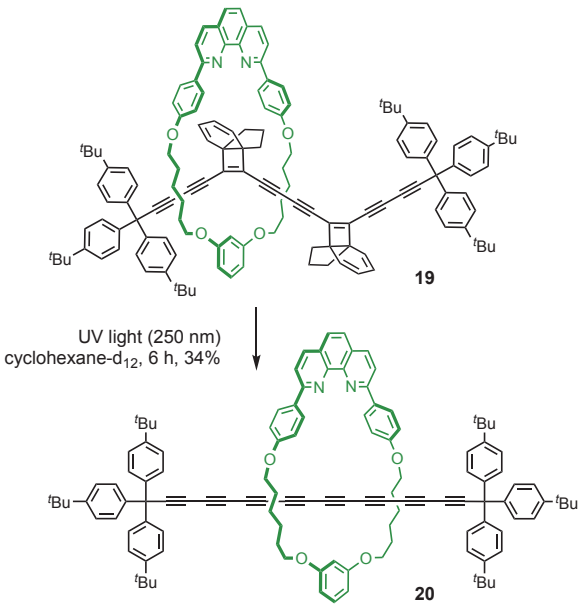

Figure 25. Photochemical unmasking of a polyyne rotaxane.[94]

It seems unlikely that any cyclo[*n*]carbons are stable enough to be isolated in the pure crystalline state under ambient conditions, because when two cyclo[*n*]carbon molecules come together they probably react to generate a cross-linked polymer, in a similar manner to long linear polyynes.[105] Tykwinski and co-workers have shown that linear polyynes can be stabilized by adding bulky end groups, with examples up to linear-C_{48}.[106] Another strategy for stabilizing linear polyynes is supramolecular encapsulation: threading polyynes through macrocycles to form rotaxanes significantly increases their thermal stability.[107,108] This implies that it should be possible to stabilize cyclo[*n*]carbons by synthesizing them as catenanes, interlocked by protective macrocycles. This idea is inspired by work from Cram and Warmuth showing that cyclobutadiene and *ortho*-benzyne can be stabilized by supramolecular encapsulation.[109–111] Recent research in Oxford has attempted to access cyclocarbon catenanes using the MAEs developed by Tobe's group. Rotaxane **16** was prepared using active metal template synthesis,[107] then cyclooligomerized by Glaser coupling to give the masked cyclocarbon [3]catenane **17** as a complex mixture of diastereomers (Figure 24).[95] The indane moities in **16** are functionalized with bulky *t*-butyl groups to prevent the macrocycle from slipping off. The photochemical conversion of **17** to the cyclocarbon catenane **18** has not yet been achieved and test reactions indicated that the MAE does not unmask cleanly enough for this application, even in linear model systems (Figure 19b).[95] However experiments with a different photochemical MAE show that it can be unmasked in rotaxane **19** (Figure 25),[94] which suggests that similar chemistry will be effective for the synthesis of cyclocarbon catenanes. There are also promising potential routes to cyclocarbon catenanes via organometallic alkyne complexes.[87,112] In the gas phase, large cyclocarbons, such as the C_{32} ring in **18**, are unstable with respect to the formation of bicyclic, polycyclic or fullerene structures (Figure 12), however catenation by suitable macrocycles should prevent both intramolecular and intermolecular crosslinking reactions. Such large cyclocarbons are not significantly strained, and they may be no less stable than the linear polyynes developed by Tykwinski and co-workers.[106]

A different perspective on the behavior of cyclo[*n*]carbons can be gained from aberration-corrected transmission electron microscope (TEM) images of single layers of graphene (Figure 26).[113] As carbon atoms are removed by the electron beam to leave a narrow graphene nanoribbon, this ribbon abruptly springs open into a loop of linearly bonded carbon atoms, which is essentially a cyclo[*n*]carbon grafted between the edges of the graphene sheet. This process appears to be a type of retro-Bergman rearrangement (Figure 26e), and it is similar to the formation of a polyyne from a polycyclic carbon fragment shown in Figure 16. Roskamp, Jarrold and co-workers suggested a similar mechanism for the conversion of cyclocarbons into fullerenes.[114] It will be fascinating to investigate charge transport through 'double-wire' junctions of the type shown in Figure 26b, to explore quantum interference between the two pathways.[115] The fact that TEM images of edge-grafted cyclocarbons can be recorded at room temperature shows that these molecules are not limited to gas-phase or cryogenic environments. As we learn how to control the reactivity of cyclocarbons, they will open new avenues of fundamental and technological research, and they will become an increasingly important family of carbon allotropes.

Our work in the field of cyclocarbon chemistry was funded by the Leverhulme Trust (project grant RPG-2017-032) and the European Research Council (Advanced Grant 320969). We are grateful to Professor David Tew for valuable discussion and for calculating the Walsh diagram in Figure 8a.

List of Abbreviations (see also note under Table 1 on abbreviations for theoretical techniques).

AFM atomic force microscopy
BAA bond angle alternation

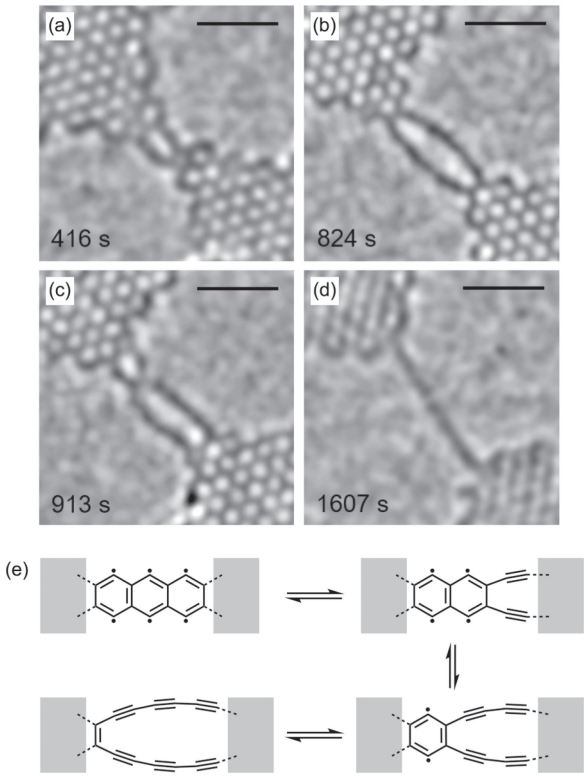

Figure 26. Aberration-corrected TEM images of an electron beam sculptured graphene nanoribbon. Images (a)–(d) were recorded as carbon atoms were gradually removed by the electron beam, showing how the constriction reconstructs into a grafted cyclocarbon, then breaks to leave a single polyyne chain. Times when the images were taken are indicated at the bottom of each frame. The scale bar in each panel is 1 nm. (e) Shows the proposed mechanism for the reconstruction. Adapted with permission from ref. 113a. Copyright 2019 American Chemical Society.

BLA	bond length alternation
DFT	density functional theory
IR	infrared
MAE	masked alkyne equivalent
R2C2PI	resonant two-color two-photon ionization
TEM	transmission electron microscopy
UPS	ultraviolet photoelectron spectroscopy
UV	ultraviolet

References

Dedicated to Professor Eiichi Nakamura on the occasion of his 70th birthday.

1 R. Hoffmann, A. A. Kabanov, A. A. Golov, D. M. Proserpio, *Angew. Chem., Int. Ed.* **2016**, *55*, 10962.

2 A. Hirsch, *Nat. Mater.* **2010**, *9*, 868.

3 F. Diederich, *Nature* **1994**, *369*, 199.

4 a) G. Li, Y. Li, H. Liu, Y. Guo, Y. Li, D. Zhu, *Chem. Commun.* **2010**, *46*, 3256. b) R. Matsuoka, R. Sakamoto, K. Hoshiko, S. Sasaki, H. Masunaga, K. Nagashio, H. Nishihara, *J. Am. Chem. Soc.* **2017**, *139*, 3145.

5 a) R.-S. Zhang, J.-W. Jiang, *Front. Phys.* **2019**, *14*, 13401. b) M. Esser, A. A. Esser, D. M. Proserpio, R. Dronskowski, *Carbon* **2017**, *121*, 154.

6 a) A. L. Mackay, H. Terrones, *Nature* **1991**, *352*, 762. b) H. Weng, Y. Liang, Q. Xu, R. Yu, Z. Fang, X. Dai, Y. Kawazoe, *Phys. Rev. B: Condens. Matter Mater. Phys.* **2015**, *92*, 045108.

7 a) Y. Segawa, D. R. Levine, K. Itami, *Acc. Chem. Res.* **2019**, *52*, 2760. b) S. H. Pun, Q. Miao, *Acc. Chem. Res.* **2018**, *51*, 1630.

8 a) W. Weltner, Jr., R. J. Van Zee, *Chem. Rev.* **1989**, *89*, 1713. b) A. Van Orden, R. J. Saykally, *Chem. Rev.* **1998**, *98*, 2313. c) C. Lifshitz, *Int. J. Mass Spectrom.* **2000**, *200*, 423.

9 a) M. C. McCarthy, P. Thaddeus, *Chem. Soc. Rev.* **2001**, *30*, 177. b) L. N. Zack, J. P. Maier, *Chem. Soc. Rev.* **2014**, *43*, 4602. c) J. P. Maier, E. K. Campbell, *Angew. Chem., Int. Ed.* **2017**, *56*, 4920.

10 J. D. Shea, *Phys. Rev.* **1927**, *30*, 825.

11 a) R. S. Richardson, *Astrophys. J.* **1931**, *73*, 216. b) J. G. Fox, G. Herzberg, *Phys. Rev.* **1937**, *52*, 638.

12 O. Hahn, F. Strassmann, J. Mattauch, H. Ewald, *Naturwissenschaften* **1942**, *30*, 541.

13 a) E. A. Rohlfing, D. M. Cox, A. Kaldor, *J. Chem. Phys.* **1984**, *81*, 3322. b) H. Y. So, C. L. Wilkins, *J. Phys. Chem.* **1989**, *93*, 1184.

14 H. W. Kroto, J. R. Heath, S. C. O'Brien, R. F. Curl, R. E. Smalley, *Nature* **1985**, *318*, 162.

15 W. Krätschmer, L. D. Lamb, K. Fostiropoulos, D. R. Huffman, *Nature* **1990**, *347*, 354.

16 a) S. W. McElvany, W. R. Creasy, A. O'Keefe, *J. Chem. Phys.* **1986**, *85*, 632. b) S. W. McElvany, B. I. Dunlap, A. O'Keefe, *J. Chem. Phys.* **1987**, *86*, 715. c) S. W. McElvany, *J. Chem. Phys.* **1988**, *89*, 2063. d) D. C. Parent, S. W. McElvany, *J. Am. Chem. Soc.* **1989**, *111*, 2393.

17 S. Yang, K. J. Taylor, M. J. Craycraft, J. Conceicao, C. L. Pettiette, O. Cheshnovsky, R. E. Smalley, *Chem. Phys. Lett.* **1988**, *144*, 431.

18 G. von Helden, M.-T. Hsu, P. R. Kemper, M. T. Bowers, *J. Chem. Phys.* **1991**, *95*, 3835.

19 F. Diederich, Y. Rubin, C. B. Knobler, R. L. Whetten, K. E. Schriver, K. N. Houk, Y. Li, *Science* **1989**, *245*, 1088.

20 K. Kaiser, L. M. Scriven, F. Schulz, P. Gawel, L. Gross, H. L. Anderson, *Science* **2019**, *365*, 1299.

21 L. M. Scriven, K. Kaiser, F. Schulz, A. J. Sterling, S. L. Woltering, P. Gawel, K. E. Christensen, H. L. Anderson, L. Gross, *J. Am. Chem. Soc.* **2020**, *142*, 12921.

22 For an earlier review of cyclocarbons see: Y. Tobe, T. Wakabayashi, In *Polyynes: Synthesis, Properties, and Applications*; F. Cataldo, Ed.; CRC Press/Taylor & Francis: Boca Raton, 2006; p. 99.

23 S. W. McElvany, M. M. Ross, N. S. Goroff, F. Diederich, *Science* **1993**, *259*, 1594.

24 a) J. Hunter, J. Fye, M. E. Jarrold, *Science* **1993**, *260*, 784. b) N. S. Goroff, *Acc. Chem. Res.* **1996**, *29*, 77.

25 G. von Helden, N. G. Gotts, M. T. Bowers, *Nature* **1993**, *363*, 60.

26 K. S. Pitzer, E. Clementi, *J. Am. Chem. Soc.* **1959**, *81*, 4477.

27 J. Chandrasekhar, E. D. Jemmis, P. v. R. Schleyer, *Tetrahedron Lett.* **1979**, *20*, 3707.

28 P. W. Fowler, N. Mizoguchi, D. E. Bean, R. W. A. Havenith, *Chem.—Eur. J.* **2009**, *15*, 6964.

29 R. Hoffmann, *Tetrahedron* **1966**, *22*, 521.

30 J. Hutter, H. P. Lüthi, F. Diederich, *J. Am. Chem. Soc.* **1994**, *116*, 750.

31 J. M. L. Martin, P. R. Taylor, *J. Phys. Chem.* **1996**, *100*,

6047.
32 T. W. Yen, S. K. Lai, *J. Chem. Phys.* **2015**, *142*, 084313.
33 K. Remya, C. H. Suresh, *RSC Adv.* **2016**, *6*, 44261.
34 B. G. A. Brito, G.-Q. Hai, L. Cândido, *Phys. Rev. A* **2018**, *98*, 062508.
35 D. Manna, J. M. L. Martin, *J. Phys. Chem. A* **2016**, *120*, 153.
36 R. O. Jones, *J. Chem. Phys.* **1999**, *110*, 5189.
37 a) V. Parasuk, J. Almlöf, *Chem. Phys. Lett.* **1991**, *184*, 187. b) H. Prinzbach, A. Weiler, P. Landenberger, F. Wahl, J. Wörth, L. T. Scott, M. Gelmont, D. Olevano, B. v. Issendorff, *Nature* **2000**, *407*, 60.
38 M. Feyereisen, M. Gutowski, J. Simons, J. Almlöf, *J. Chem. Phys.* **1992**, *96*, 2926.
39 S. Maeda, K. Ohno, *J. Chem. Phys.* **2006**, *124*, 174306.
40 D. M. Cleland, E. K. Fletcher, A. Kuperman, M. C. Per, *J. Phys.: Mater.* **2020**, *3*, 025006.
41 S. R. Marder, L.-T. Cheng, B. G. Tiemann, A. C. Friedli, M. Blanchard-Desce, J. W. Perry, J. Skindhøj, *Science* **1994**, *263*, 511.
42 M. Saito, Y. Okamoto, *Phys. Rev. B: Condens. Matter Mater. Phys.* **1999**, *60*, 8939.
43 E. J. Bylaska, R. Kawai, J. H. Weare, *J. Chem. Phys.* **2000**, *113*, 6096.
44 D. Wendinger, R. R. Tykwinski, *Acc. Chem. Res.* **2017**, *50*, 1468.
45 L. Belau, S. E. Wheeler, B. W. Ticknor, M. Ahmed, S. R. Leone, W. D. Allen, H. F. Schaefer, M. A. Duncan, *J. Am. Chem. Soc.* **2007**, *129*, 10229.
46 K. Raghavachari, R. A. Whiteside, J. A. Pople, *J. Chem. Phys.* **1986**, *85*, 6623.
47 C. Liang, H. F. Schaefer, III, *J. Chem. Phys.* **1990**, *93*, 8844.
48 V. Parasuk, J. Almlöf, M. W. Feyereisen, *J. Am. Chem. Soc.* **1991**, *113*, 1049.
49 J. D. Watts, R. J. Bartlett, *Chem. Phys. Lett.* **1992**, *190*, 19.
50 D. A. Plattner, K. N. Houk, *J. Am. Chem. Soc.* **1995**, *117*, 4405.
51 J. M. L. Martin, J. El-Yazal, J.-P. François, *Chem. Phys. Lett.* **1995**, *242*, 570.
52 T. Torelli, L. Mitas, *Phys. Rev. Lett.* **2000**, *85*, 1702.
53 A. E. Boguslavskiy, H. Ding, J. P. Maier, *J. Chem. Phys.* **2005**, *123*, 034305.
54 S. Arulmozhiraja, T. Ohno, *J. Chem. Phys.* **2008**, *128*, 114301.
55 K. Remya, C. H. Suresh, *RSC Adv.* **2016**, *6*, 44261.
56 E. Brémond, A. J. Pérez-Jiménez, C. Adamo, J. C. Sancho-Garcia, *J. Chem. Phys.* **2019**, *151*, 211104.
57 G. V. Baryshnikov, R. R. Valiev, A. V. Kuklin, D. Sundholm, H. Ågren, *J. Phys. Chem. Lett.* **2019**, *10*, 6701.
58 N. D. Charistos, A. Muñoz-Castro, *Phys. Chem. Chem. Phys.* **2020**, *22*, 9240.
59 We thank David P. Tew for calculating the Walsh diagram in Figure 8a, which was computed using relaxed structures and orbital energies at the Brueckner coupled cluster doubles level of theory.[60] A similar plot was published in M. D. Wodrich, C. Corminboeuf, S. S. Park, P. von R. Schleyer, *Chem.—Eur. J.* **2007**, *13*, 4582.
60 a) N. C. Handy, J. A. Pople, M. Head-Gordon, K. Raghavachari, G. W. Trucks, *Chem. Phys. Lett.* **1989**, *164*, 185. b) D. P. Tew, *J. Chem. Phys.* **2016**, *145*, 074103.
61 J. M. L. Martin, J. El-Yazal, J.-P. François, *Chem. Phys. Lett.* **1996**, *252*, 9.
62 a) T. Bally, *Angew. Chem., Int. Ed.* **2006**, *45*, 6616. b) A. M. Orendt, B. R. Arnold, J. G. Radziszewski, J. C. Facelli, K. D. Malsch, H. Strub, D. M. Grant, J. Michl, *J. Am. Chem. Soc.* **1988**, *110*, 2648. c) P. C. Varras, P. S. Gritzapis, *Chem. Phys. Lett.* **2018**, *711*, 166.
63 Z. S. Pereira, E. Z. da Silva, *J. Phys. Chem. A* **2020**, *124*, 1152.
64 A. Nandi, E. Solel, S. Kozuch, *Chem.—Eur. J.* **2020**, *26*, 625.
65 C. Castro, W. L. Karney, *Angew. Chem., Int. Ed.* **2020**, *59*, 8355.
66 a) E. Dörnenburg, H. Hintenberger, J. Franzen, *Z. Naturforsch., A* **1961**, *16*, 532. b) N. Fürstenau, F. Hillenkamp, *Int. J. Mass Spectrom.* **1981**, *37*, 135.
67 a) K. Kaizu, M. Kohno, S. Suzuki, H. Shiromaru, T. Moriwaki, Y. Achiba, *J. Chem. Phys.* **1997**, *106*, 9954. b) T. Wakabayashi, T. Momose, T. Shida, *J. Chem. Phys.* **1999**, *111*, 6260.
68 G. von Helden, P. R. Kemper, N. G. Gotts, M. T. Bowers, *Science* **1993**, *259*, 1300.
69 a) G. von Helden, M.-T. Hsu, N. G. Gotts, M. T. Bowers, *J. Phys. Chem.* **1993**, *97*, 8182. b) G. von Helden, N. G. Gotts, M. T. Bowers, *J. Am. Chem. Soc.* **1993**, *115*, 4363.
70 K. Koyasu, T. Ohtaki, J. Bing, K. Takahashi, F. Misaizu, *Phys. Chem. Chem. Phys.* **2015**, *17*, 24810.
71 A. E. Boguslavskiy, J. P. Maier, *Phys. Chem. Chem. Phys.* **2007**, *9*, 127.
72 K. R. Thompson, R. L. DeKock, W. Weltner, Jr., *J. Am. Chem. Soc.* **1971**, *93*, 4688.
73 J. Szczepanski, M. Vala, *J. Phys. Chem.* **1991**, *95*, 2792.
74 J. D. Presilla-Márquez, J. A. Sheehy, J. D. Mills, P. G. Carrick, C. W. Larson, *Chem. Phys. Lett.* **1997**, *274*, 439.
75 S. L. Wang, C. M. L. Rittby, W. R. M. Graham, *J. Chem. Phys.* **1997**, *107*, 6032.
76 S. L. Wang, C. M. L. Rittby, W. R. M. Graham, *J. Chem. Phys.* **1997**, *107*, 7025.
77 J. D. Presilla-Márquez, J. Harper, J. A. Sheehy, P. G. Carrick, C. W. Larson, *Chem. Phys. Lett.* **1999**, *300*, 719.
78 a) A. K. Ott, G. A. Rechtsteiner, C. Felix, O. Hampe, M. F. Jarrold, R. P. Van Duyne, *J. Chem. Phys.* **1998**, *109*, 9652. b) G. A. Rechtsteiner, C. Felix, A. K. Ott, O. Hampe, R. P. Van Duyne, M. F. Jarrold, K. Raghavachari, *J. Phys. Chem. A* **2001**, *105*, 3029.
79 M. Grutter, M. Wyss, E. Riaplov, J. P. Maier, *J. Chem. Phys.* **1999**, *111*, 7397.
80 a) C. Lifshitz, T. Peres, S. Kababia, I. Agranat, *Int. J. Mass Spectrom. Ion Processes* **1988**, *82*, 193. b) C. Lifshitz, T. Peres, I. Agranat, *Int. J. Mass Spectrom. Ion Processes* **1989**, *93*, 149. c) J. Sun, H.-F. Grützmacher, C. Lifshitz, *J. Am. Chem. Soc.* **1993**, *115*, 8382. d) C. Lifshitz, P. Sandler, H.-F. Grützmacher, J. Sun, T. Weiske, H. Schwarz, *J. Phys. Chem.* **1993**, *97*, 6592. e) J. Sun, H.-F. Grützmacher, C. Lifshitz, *Int. J. Mass Spectrom. Ion Processes* **1994**, *138*, 49.
81 G. von Helden, E. Porter, N. G. Gotts, M. T. Bowers, *J. Phys. Chem.* **1995**, *99*, 7707.
82 J. Fulara, E. Riaplov, A. Batalov, I. Shnitko, J. P. Maier, *J. Chem. Phys.* **2004**, *120*, 7520.
83 F. Diederich, Y. Rubin, *Angew. Chem., Int. Ed. Engl.* **1992**, *31*, 1101.
84 F. Diederich, Y. Rubin, O. L. Chapman, N. S. Goroff, *Helv. Chim. Acta* **1994**, *77*, 1441.
85 Y. Rubin, C. B. Knobler, F. Diederich, *J. Am. Chem. Soc.*

1990, *112*, 1607.
86 Y. Rubin, M. Kahr, C. B. Knobler, F. Diederich, C. L. Wilkins, *J. Am. Chem. Soc.* **1991**, *113*, 495.
87 Y. Rubin, C. B. Knobler, F. Diederich, *J. Am. Chem. Soc.* **1990**, *112*, 4966.
88 Y. Rubin, S. S. Lin, C. B. Knobler, J. Anthony, A. M. Boldi, F. Diederich, *J. Am. Chem. Soc.* **1991**, *113*, 6943.
89 T.-M. Chang, A. Naim, S. N. Ahmed, G. Goodloe, P. B. Shevlin, *J. Am. Chem. Soc.* **1992**, *114*, 7603.
90 G. A. Adamson, C. W. Rees, *J. Chem. Soc., Perkin Trans. 1* **1996**, 1535.
91 C. D. Campbell, C. W. Rees, *J. Chem. Soc. C* **1969**, 742.
92 a) Y. Tobe, T. Fujii, K. Naemura, *J. Org. Chem.* **1994**, *59*, 1236. b) Y. Tobe, H. Matsumoto, K. Naemura, Y. Achiba, T. Wakabayashi, *Angew. Chem., Int. Ed. Engl.* **1996**, *35*, 1800. c) Y. Tobe, T. Fujii, H. Matsumoto, K. Naemura, Y. Achiba, T. Wakabayashi, *J. Am. Chem. Soc.* **1996**, *118*, 2758. d) Y. Tobe, T. Fujii, H. Matsumoto, K. Tsumuraya, D. Noguchi, N. Nakagawa, M. Sonoda, K. Naemura, Y. Achiba, T. Wakabayashi, *J. Am. Chem. Soc.* **2000**, *122*, 1762.
93 Y. Tobe, R. Umeda, N. Iwasa, M. Sonoda, *Chem.—Eur. J.* **2003**, *9*, 5549.
94 S. L. Woltering, P. Gawel, K. E. Christensen, A. L. Thompson, H. L. Anderson, *J. Am. Chem. Soc.* **2020**, *142*, 13523.
95 P. Gawel, S. L. Woltering, Y. Xiong, K. E. Christensen, H. L. Anderson, *Angew. Chem., Int. Ed.*, doi:10.1002/anie.202013623.
96 T. Wakabayashi, M. Kohno, Y. Achiba, H. Shiromaru, T. Momose, T. Shida, K. Naemura, Y. Tobe, *J. Chem. Phys.* **1997**, *107*, 4783.
97 N. Pavliček, B. Schuler, S. Collazos, N. Moll, D. Pérez, E. Guitián, G. Meyer, D. Peña, L. Gross, *Nat. Chem.* **2015**, *7*, 623.
98 a) N. Pavliček, P. Gawel, D. R. Kohn, Z. Majzik, Y. Xiong, G. Meyer, H. L. Anderson, L. Gross, *Nat. Chem.* **2018**, *10*, 853. b) B. Schuler, W. Liu, A. Tkatchenko, N. Moll, G. Meyer, A. Mistry, D. Fox, L. Gross, *Phys. Rev. Lett.* **2013**, *111*, 106103.
99 L. Gross, F. Mohn, N. Moll, P. Liljeroth, G. Meyer, *Science* **2009**, *325*, 1110.
100 a) D. M. Eigler, E. K. Schweizer, *Nature* **1990**, *344*, 524. b) B. C. Stipe, M. A. Rezaei, W. Ho, S. Gao, M. Persson, B. I. Lundqvist, *Phys. Rev. Lett.* **1997**, *78*, 4410. c) S.-W. Hla, L. Bartels, G. Meyer, K.-H. Rieder, *Phys. Rev. Lett.* **2000**, *85*, 2777. d) Y. Kim, T. Komeda, M. Kawai, *Phys. Rev. Lett.* **2002**, *89*, 126104.
101 N. Pavliček, L. Gross, *Nat. Rev. Chem.* **2017**, *1*, 0005.
102 a) L. Gross, B. Schuler, N. Pavliček, S. Fatayer, Z. Majzik, N. Moll, D. Peña, G. Meyer, *Angew. Chem., Int. Ed.* **2018**, *57*, 3888. b) B. Schuler, S. Fatayer, F. Mohn, N. Moll, N. Pavliček, G. Meyer, D. Peña, L. Gross, *Nat. Chem.* **2016**, *8*, 220.
103 M. Li, Z. Gao, Y. Han, Y. Zhao, K. Yuan, S. Nagase, M. Ehara, X. Zhao, *Phys. Chem. Chem. Phys.* **2020**, *22*, 4823.
104 S. Schrettl, C. Stefaniu, C. Schwieger, G. Pasche, E. Oveisi, Y. Fontana, A. Fontcuberta i Morral, J. Reguera, R. Petraglia, C. Corminboeuf, G. Brezesinski, H. Frauenrath, *Nat. Chem.* **2014**, *6*, 468.
105 T. R. Hoye, B. Baire, D. Niu, P. H. Willoughby, B. P. Woods, *Nature* **2012**, *490*, 208.
106 a) Y. Gao, Y. Hou, F. Gordillo Gámez, M. J. Ferguson, J. Casado, R. R. Tykwinski, *Nat. Chem.* **2020**, *12*, 1143. b) W. Chalifoux, R. R. Tykwinski, *Nat. Chem.* **2010**, *2*, 967.
107 a) L. D. Movsisyan, M. Franz, F. Hampel, A. L. Thompson, R. R. Tykwinski, H. L. Anderson, *J. Am. Chem. Soc.* **2016**, *138*, 1366. b) L. D. Movsisyan, D. V. Kondratuk, M. Franz, A. L. Thompson, R. R. Tykwinski, H. L. Anderson, *Org. Lett.* **2012**, *14*, 3424. c) N. Weisbach, Z. Baranova, S. Gauthier, J. H. Reibenspies, J. A. Gladysz, *Chem. Commun.* **2012**, *48*, 7562.
108 S. Schrettl, E. Contal, T. N. Hoheisel, M. Fritzsche, S. Balog, R. Szilluweit, H. Frauenrath, *Chem. Sci.* **2015**, *6*, 564.
109 D. J. Cram, M. E. Tanner, R. Thomas, *Angew. Chem., Int. Ed. Engl.* **1991**, *30*, 1024.
110 R. Warmuth, *Angew. Chem., Int. Ed. Engl.* **1997**, *36*, 1347.
111 a) A. Galan, P. Ballester, *Chem. Soc. Rev.* **2016**, *45*, 1720. b) M. J. Frampton, H. L. Anderson, *Angew. Chem., Int. Ed.* **2007**, *46*, 1028.
112 D. R. Kohn, P. Gawel, Y. Xiong, K. E. Christensen, H. L. Anderson, *J. Org. Chem.* **2018**, *83*, 2077.
113 a) J. K. Lee, G.-D. Lee, S. Lee, E. Yoon, H. L. Anderson, G. A. D. Briggs, J. H. Warner, *ACS Nano* **2019**, *13*, 2379. b) Y.-C. Lin, S. Morishita, M. Koshino, C.-H. Yeh, P.-Y. Teng, P.-W. Chiu, H. Sawada, K. Suenaga, *Nano Lett.* **2017**, *17*, 494. c) Y. Rong, J. H. Warner, *ACS Nano* **2014**, *8*, 11907.
114 J. M. Hunter, J. L. Fye, E. J. Roskamp, M. F. Jarrold, *J. Phys. Chem.* **1994**, *98*, 1810.
115 a) H. Vazquez, R. Skouta, S. Schneebeli, M. Kamenetska, R. Breslow, L. Venkataraman, M. S. Hybertsen, *Nat. Nanotechnol.* **2012**, *7*, 663. b) S. Richert, J. Cremers, I. Kuprov, M. D. Peeks, H. L. Anderson, C. R. Timmel, *Nat. Commun.* **2017**, *8*, 14842.

